JACS
JOURNAL OF THE AMERICAN CHEMICAL SOCIETY

Editors' Choice

pubs.acs.org/JACS

Article

One-step Formation of Urea from Carbon Dioxide and Nitrogen Using Water Microdroplets

Xiaowei Song,[‖] Chanbasha Basheer,*[,‖] Yu Xia, Juan Li, Ismail Abdulazeez, Abdulaziz A. Al-Saadi, Mohammad Mofidfar, Mohammed Altahir Suliman, and Richard N. Zare*

Cite This: *J. Am. Chem. Soc.* 2023, 145, 25910−25916

Read Online

ACCESS | Metrics & More | Article Recommendations | Supporting Information

ABSTRACT: Water (H_2O) microdroplets are sprayed onto a graphite mesh covered with a $CuBi_2O_4$ coating using a 1:1 mixture of N_2 and CO_2 as the nebulizing gas. The resulting microdroplets contain urea [$CO(NH_2)_2$] as detected by both mass spectrometry and ^{13}C nuclear magnetic resonance. This gas−liquid−solid heterogeneous catalytic system synthesizes urea in one step on the 0.1 ms time scale. The conversion rate reaches 2.7 mmol g^{-1} h^{-1} at 25 °C and 12.3 mmol g^{-1} h^{-1} at 65 °C, with no external voltage applied. Water microdroplets serve as the hydrogen source and the electron transfer medium for N_2 and CO_2 in contact with $CuBi_2O_4$. Water−gas and water−solid contact electrification are speculated to drive the reaction process. This strategy couples N_2 fixation and CO_2 utilization in an ecofriendly process to produce urea, converting a greenhouse gas into a value-added product.

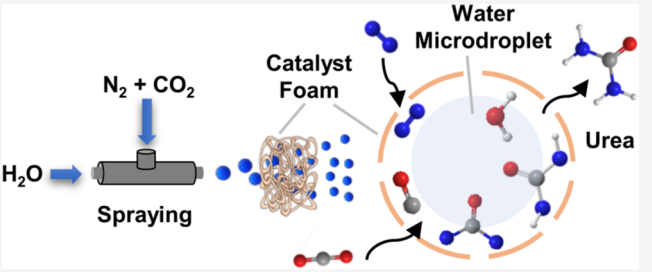

INTRODUCTION

Urea [$CO(NH_2)_2$] is the first organic molecule successfully synthesized in the laboratory, opening the field of organic chemistry. Today, over 190 million tons per year of urea are produced as fertilizer.[1] This is accomplished by adding liquified carbon dioxide (CO_2) to liquid ammonia (NH_3) under harsh conditions (400−500 K and 150−250 bar).[2] The use of high temperatures has the drawback of easily introducing degradation and unwanted byproducts such as biuret, cyanuric acid, ammelide, ammeline, and melamine.[3] Ammonia is synthesized from nitrogen (N_2) and hydrogen (H_2) by the Haber-Bosch process under high pressure and high-temperature conditions (100−200 psi, 400−500 °C), which is sufficient to break the N≡N triple bond (941 kJ mol^{-1}).[4,5] This process accounts for more than 2% of the global energy consumption.[6] The hydrogen comes from a petroleum source (methane) by reaction with steam, adding to the negative environmental impact through the release of about 1% of the carbon dioxide found in the atmosphere. Viable urea synthetic approaches under milder conditions are widely being sought to reduce environmental pollution from the present industrial process

Extensive efforts have been put into developing new functional molecules and materials for heterogeneous photo-/electrocatalytic reduction to yield urea. Metal oxides (e.g., TiO_2, Fe_2O_3, and Bi_2O_3),[7−9] metal borides (e.g., Mo_2B_2, Cr_2B_2),[10] and metal complexes (e.g., tetrahexahedral Au and iron phthalocyanine)[11,12] are prepared in various nanomaterials as catalytic electrodes. A copper bismuth oxide has been previously reported to synthesize urea electrochemically.[13,14] Recently, Pd/Cu alloy nanoparticles on TiO_2 nanosheets were reported to be an effective electrocatalyst that can produce urea from N_2 and CO_2 dissolved in H_2O with a formation rate of 3.36 mmol g^{-1} h^{-1}, which appears to be a remarkable breakthrough in green urea synthesis.[15] However, the poor solubility of N_2 in water and the postseparation of NH_3 from the aqueous electrolyte complicate the subsequent steps of urea synthesis.

Water can serve as one of the cleanest natural sources on earth for N_2 fixing and for the recycling of CO_2 from the air. Physically, spraying water microdroplets sized at around 10 μm can gain a 10,000 times larger contacting interface than the equal volume of bulk water. Therefore, water microdroplets facilitate the incorporation of the gas-phase substrates into a heterogeneous reaction system by sufficient contact with a solid catalyst, increasing the catalytic performance rather than being dissolved in a bulk solution. Recently, we have demonstrated how nitrogen can be converted to ammonia using water microdroplets combined with a catalyst.[16] These issues motivated us to search for a simpler reaction system beyond the conventional paradigm of photo/electrocatalysis for making urea.

Received: September 29, 2023
Revised: October 11, 2023
Accepted: October 13, 2023
Published: November 15, 2023

https://doi.org/10.1021/jacs.3c10784
J. Am. Chem. Soc. 2023, 145, 25910−25916

EXPERIMENTAL SECTION

Figure 1 presents the experimental setup for urea production. Water microdroplets are sprayed with a 1:1 mixture of N_2 and CO_2 as nebulizing gas. The microdroplets strike a graphite mesh coated with $CuBi_2O_4$ and pass through the mesh, where they are analyzed with a mass spectrometer (Figure S1). The $CuBi_2O_4$ catalyst is synthesized by a one-step hydrothermal reaction.[17] The system represents a gas−liquid−solid heterogeneous catalytic system for producing urea.

As starting materials, CO_2 and N_2 were first fed into the triphase catalysis system from cylinders containing the compressed gases. The copper bismuth oxide catalyst was characterized by transmission electron microscopy and X-ray diffraction (Figure S2). More detailed information about the experimental conditions is presented in the Supporting Information.

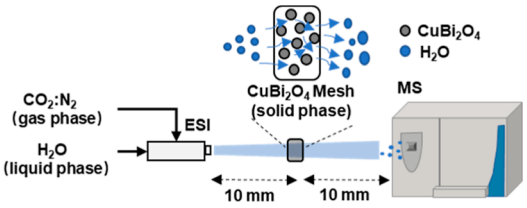

Figure 1. Schematic diagram of the sonic spraying apparatus and mass spectrometer.

RESULTS AND DISCUSSION

As an initial condition, zero external voltage was applied to the catalyst mesh and the sonic sprayer. Several urea-associated peaks can be observed in the mass spectrum (Figure 2a). Apart from the urea monomer ion (m/z 61, $[\text{urea} + \text{H}]^+$; m/z 83, $[\text{urea} + \text{Na}]^+$), the generated urea also exists as forms of a dimer (m/z 121, $[2\text{urea} + \text{H}]^+$; m/z 143, $[2\text{urea} + \text{Na}]^+$) due to the intermolecular hydrogen bonding, which may indicate a considerable urea yield. In addition, the existence of an ammonium-adducted urea peak (m/z 78, $[\text{urea} + \text{NH}_4]^+$) revealed that ammonia is also generated as a byproduct in the synthesis of urea. Based on its ion intensity, this ammonia accounted for approximately 12% of the total amount of urea. Apart from the final product, urea, two adsorbed intermediates $[\text{NCON} + \text{H}]^+$ (m/z 57) and $[\text{HNCONH} + \text{H}]^+$ (m/z 59) were also detected in the mass spectrum, which will be further discussed in proposing a mechanism.

However, when replacing the water flow with methanol, urea-associated MS signals gradually disappeared (Figure S3a). This negative control illustrates the critical role of water microdroplets in the formation of urea as the source of reduced protons and free electrons. When the CO_2 gas supply was stopped, and the native CO_2 dissolved in water was completely removed, there was also no urea-associated peak observed (Figure S3b). Apart from water microdroplets, the surface hydrophobicity of the graphite support is another contributing factor that could influence urea production. When we replaced the mesh of hydrophobic graphite with a hydrophilic copper foam, only a weak urea signal could be observed from the mass spectrum (Figure S3c). The atomized water microdroplets may be recondensed into the bulk form when passing through the hydrophilic porous medium. It not only shortens the survival time of microdroplets but also suppresses the ionization of the urea product. In contrast, a hydrophobic medium (contact angle 113°, Figure S4) can make sprayed microdroplets survive in a higher amount and a longer period because of the weak surface tension between liquid and solid phases.

We also investigated the use of compressed air containing 78% N_2 as the nitrogen source, as well as using CO_2 dissolved in the water. We found that the urea abundance was not seriously affected by the less pure starting N_2 and by the physical status of CO_2 (Figure 2b,c). These results demonstrate the robustness of the proposed heterogeneous catalysis system. It also provided promising potential for selecting more widely available starting materials for urea

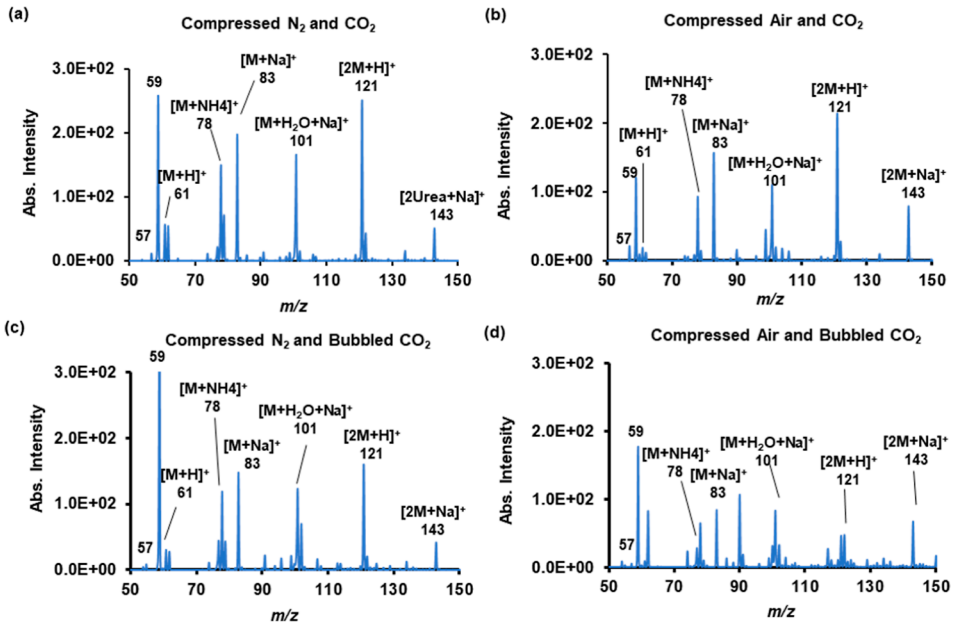

Figure 2. Real-time monitoring of the urea generation process by spraying water microdroplets and the $CuBi_2O_4$ catalyst. (a) N_2 and CO_2 as the nebulizing gases to spray water microdroplets onto the $CuBi_2O_4$ catalyst coated on a hydrophobic mesh; (b) N_2 and CO_2 as the nebulizing gases to spray water microdroplets onto the $CuBi_2O_4$ catalyst coated on a hydrophilic mesh; (c) N_2 and CO_2 were directly sprayed onto the $CuBi_2O_4$ catalyst with no spraying water microdroplets; (d) N_2 was replaced by the compression air to conduct the urea synthesis.

https://doi.org/10.1021/jacs.3c10784
J. Am. Chem. Soc. 2023, 145, 25910−25916

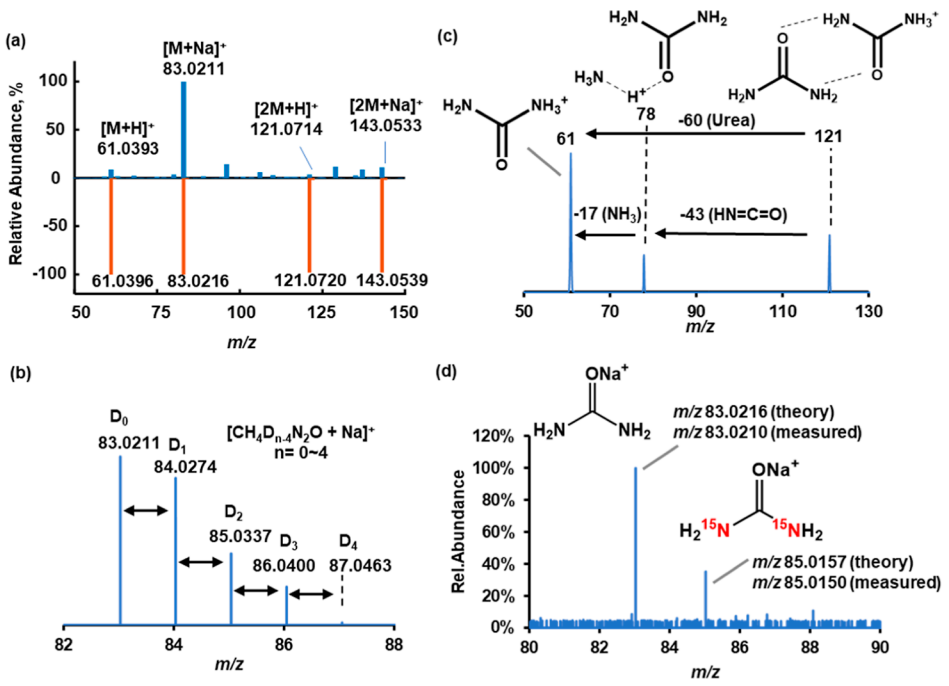

Figure 3. Identification of the generated urea product. (a) Exact m/z matching of the high-resolution mass spectrum; (b) confirmation of the number of active proton sites by HDX-MS; (c) structural elucidation by the MS/MS experiment; and (d) high-resolution mass spectrum of native and ^{15}N-labeled urea formed by using the nebulizing gas mixture of $^{14}N_2$ and $^{15}N_2$.

synthesis. When simultaneously feeding compressed air and bubbling CO_2 into water, the urea mass peak suffered some loss in intensity, but major urea-associated peaks can be successfully observed in the mass spectrum (Figure 2d).

The identity of urea was verified by high-resolution mass spectrometry, hydrogen−deuterium exchange mass spectrometry (HDX-MS), and tandem mass spectrometry (MS/MS). The exact values for urea-associated ions were also measured to be within the acceptable mass tolerance of 5.0 ppm by comparison with their theoretical m/z values (Figure 3a). HDX-MS successfully confirmed the four active protons located in the two amine groups, ruling out other possible interfering agents derived from isobaric ions (Figure 3b). MS/MS was conducted on the predominant urea species (m/z 121, $[2M + H]^+$) through collision-induced dissociation (CID). We observed a fragment ion of $[urea + H]^+$ (m/z 61), $[urea + NH_4]^+$ (m/z 78), and neutral losses of 43 (HNCO), 17 (NH_3), and 60 (urea) (Figure 3c). This pattern matched the CID spectrum collected from the urea standard. Additionally, the urea was further confirmed by testing the off-line collected sample with ^{13}C nuclear magnetic resonance (Figure S5).

To further confirm that the source of nitrogen in the urea we form arises from N_2 in the nebulizing gas and not from some other nitrogen source, we substituted ^{15}N-labeled N_2 in the nebulizing gas and observed that the resulting urea was isotopically labeled (Figure 3d). Conditions of spraying were optimized to obtain the highest urea concentration. It was found that the urea concentration can reach the highest concentration of 2.8 ± 0.3 μM without an applied external potential (Figure S6). This is a striking phenomenon because it means that the proposed triphase catalysis can be self-powered compared to conventional electrocatalysis. The urea conversion rates were also estimated. During the whole reaction process, 500 μL of water was fed at a flow rate of 10 μL/min and completely consumed within 0.8 h. The spray impact region was around 1 cm^2 on the 2×10^{-4} g $CuBi_2O_4$ coating of the graphite mesh. Only the area of the graphite mesh being sprayed by droplets was used for calculating the urea conversion yield, which were 2.7 and 12.3 mmol h^{-1} g^{-1} at 25 and 65 °C, respectively. This system is able to produce directly the final urea product at a rate per gram of catalyst per hour that exceeds the previous report of 3.36 mmol h^{-1} g^{-1}.[15]

Based on our previous work synthesizing ammonia from N_2 and water microdroplets and using density functional theory (DFT) calculations,[16] we suggest a plausible mechanism for urea synthesis. According to the previous studies for the N_2/NH_3 conversion, the N_2 absorption and activation is the first important and rate-limiting step for the following N_2 reduction.[16,17] Therefore, water microdroplets can help to increase the chance and area for physical contact between N_2 and $CuBi_2O_4$, thereby overcoming the low solubility of N_2 in aqueous solution (20 mg/L, 20 °C, 100 kPa). Once N_2 is chemically adsorbed by $CuBi_2O_4$, the N≡N triple bond will be lengthened and activated.

The positive detection of ammonia adduct (m/z 78, $[Urea + NH_4]^+$) shows an associative/dissociation mechanism-driven process.[18] We propose that water is the major source for reducing hydrogen. In previous work, electron spin resonance spectroscopy has shown that hydroxyl radicals ($^{\bullet}OH$) and hydrogen atoms ($^{\bullet}H$) are formed at the gas−water and solid−water interfaces,[19] which strongly supports the recent proposal that Colussi made for hydrogen peroxide formation on the sprayed water microdroplet surface.[20] Interestingly, the endothermicity of electron transfer in bulk water (ΔH = 448 kJ mol^{-1}) is reversed at the water interface by the destabilization of the hydrated reactant ions: ΔH hydration ($H^+ + OH^-$) = −1670 kJ mol^{-1}, relative to neutral radical products: ΔH hydration ($^{\bullet}OH + {}^{\bullet}H$) = −58 kJ mol^{-1}. This provides the necessary hydrogenation to drive the formation of NH_3 as well as NH_2CONH_2. This work has revealed that the

https://doi.org/10.1021/jacs.3c10784
J. Am. Chem. Soc. 2023, 145, 25910−25916

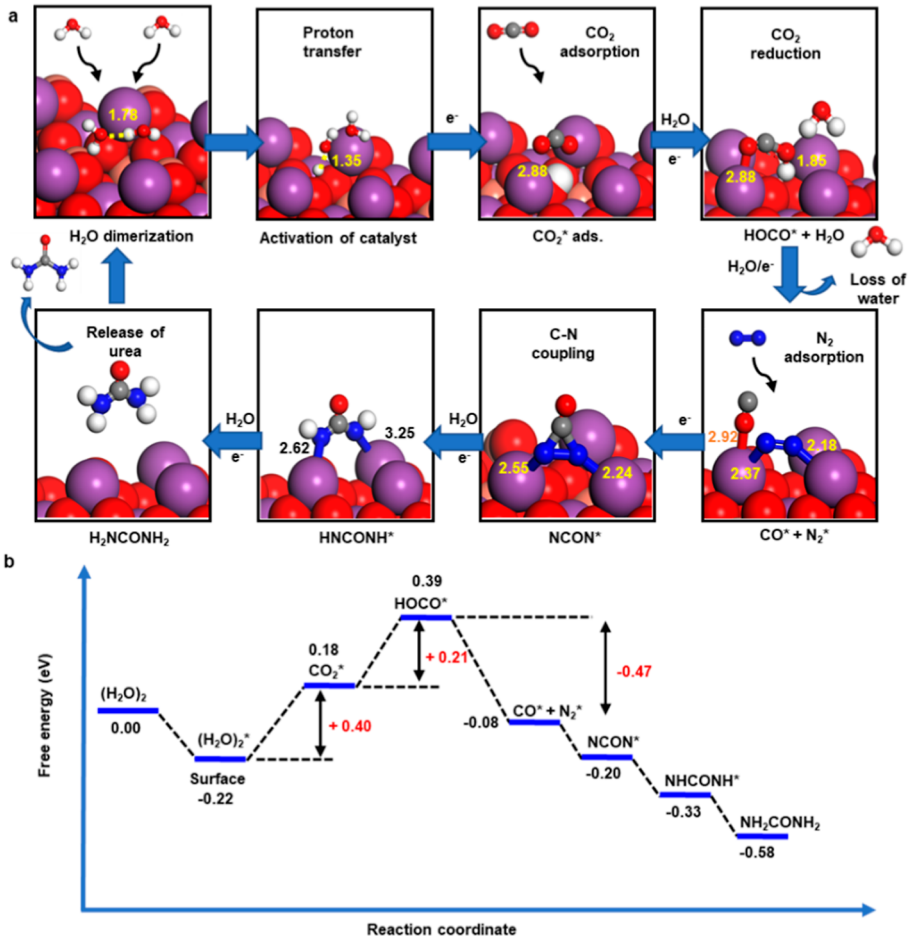

Figure 4. Urea formation process simulated by DFT: (a) Optimized structural pathway of the exclusive mechanism where purple spheres are Bi, red spheres are O, and brown spheres are Cu. Values in the figure present the bond lengths (in Å); and (b) energy profile of the electrosynthesis of urea on the $CuBi_2O_4$(211) surface, showing the concerted pathway. The free energy changes are indicated in red. The superscript asterisk represents surface adsorption.

external potential does not substantially facilitate urea production. It hinted that the driving potential for N_2/CO_2 reduction and coupling may be self-powered simply from the spraying process.

Mounting evidence has confirmed the theoretical claim about the existence of an ultrahigh electric field (10^9 V/m) across the air−water interface of microdroplets, which is sufficient to induce spontaneous redox reactions.[21,22] In addition, contact electrification between water and a solid surface is another crucial physicochemical process at water−solid interfaces.[23] Zhou, Guo, and co-workers even observed an electrical current of 380 nA and sustained voltage of up to 1 V generated from the water evaporation through the surface of nanostructured carbon materials under ambient conditions.[24] Under high pressure (120 psi) and rapid relative movement (80 m/s), it was shown that the catalyst mesh could be charged with negative current as high as −200 pA (Figure S7) by contact electrification when it was sprayed by our presented system simultaneously involving liquid (H_2O), gas (CO_2 and N_2), and solid phases ($CuBi_2O_4$). Contact electrification between water−solid, water−gas, and solid−gas causes interfacial charge/electron transfer and separation.[25] Extremely close contact between any of the above two phases may also generate a strong static electric field to drive the C−N coupling and redox reaction. In general, spraying water microdroplets provided a very special physiochemical environment to promote urea formation under no external photo/electrocatalytic conditions.

From the chemical aspect, mounting evidence in the previous studies shows that the water microdroplet interface has spontaneous redox ability driven by its unique physicochemical properties such as the interfacial electric field, orientated molecular alignment, partial solvation, spontaneous redox, and contact electrification between the liquid−solid interface, etc.[26−29]

Given the above rationales, it is expected that water microdroplets serve not only as the interaction medium that bridges the gas phase substrate and solid phase catalyst but also as proton and electron donors for nitrogen hydrogenation and urea synthesis. The ability of water microdroplets to donate electrons has been recognized previously.[30−34] This system is special in that it involves the simultaneous reaction of reagents in the gas, liquid, and solid state.

Theoretical insights into the mechanism of the C−N coupling reaction leading to the formation of urea on the $CuBi_2O_4$ heterostructure were obtained using DFT calculations. Two competing pathways were identified: the concerted pathway, in which both gases adsorb on the catalyst surface simultaneously, and the exclusive pathway, in which the gases adsorb independently. Figures 4 and S8 present the

https://doi.org/10.1021/jacs.3c10784
J. Am. Chem. Soc. 2023, 145, 25910−25916

geometrically optimized pathways and the corresponding energy profile of the reactions.

An in-depth examination of the energy pathways revealed that water dimers on the surface of the heterostructure afforded the transfer of protons and facile activation of the surface, which triggers the adsorption of CO_2 molecules in the rate-limiting step. Consequently, the CO_2 molecules bind strongly to the $CuBi_2O_4$ surface with an adsorption energy (E_{ads}) of −58.5 kJ/mol and a Bi−O binding distance of 2.88 Å. Additionally, the adsorbed CO_2 appeared distorted, with an elongation of the C = O bond by 0.03 with respect to the estimated distance in an isolated CO_2 molecule in the gas phase. Moreover, the associated water droplet forms an intermolecular hydrogen bond via the elongated oxygen atom, suggesting the facile protonation of the CO_2 and the successive hydrogenation to HOCO. Thus, the energy barrier ($E_{barrier}$) for the first hydrogenation of CO_2 to HOCO was estimated to be 0.21 eV uphill.

The next critical step is the simultaneous reduction of HOCO to CO and the adsorption of N_2 molecules in the heterostructure. The energetics of this step revealed that the catalyst surface exhibited strong binding affinity to the N_2 molecules and weakly binds to CO. The former resulted in Bi−N binding distances of 2.37 and 2.18 Å, while the latter yielded a Bi−O distance of 2.92 Å (Figure 4a). The calculated $E_{barrier}$ showed that the $CuBi_2O_4(211)$ surface rapidly catalyzes this step, resulting in the free energy change of −0.08 eV, which represents a drop of 0.47 eV.[35] The successive in situ C−N coupling reaction and the subsequent hydrogenation to urea occur spontaneously on the $CuBi_2O_4(211)$ surface due to the matching molecular orbitals. Meanwhile, the corresponding free energy change of this process revealed that the formation of the NCON intermediate is an exergonic process resulting in $\Delta(\Delta G)$ of −0.20 eV. According to Yuan et al., the subsequent hydrogenation of the adsorbed $(NCON)_{ads}$ intermediate occurs via two possible pathways: the alternating and the distal.[36] The $\Delta(\Delta G)$ values calculated in the present study indicate the occurrence of both pathways until complete hydrogenation and release of urea.

The alternative pathway to the production of NH_3 from the chemisorbed N_2 molecules on the surface of the catalyst is presented in Figure S7. DFT investigations revealed that although the adsorbed CO molecules bind weakly to the surface, the release of CO and the successive hydrogenation of N_2 could lead to the formation of NH_3. Accordingly, the free energy of the hydrogenation of N_2 to N_2H is estimated to be 0.26 eV uphill. In contrast, the second hydrogenation step occurs on the nonprotonated nitrogen to form *cis*-diazene with a $\Delta(\Delta G)$ of 0.34 eV. The third hydrogenation process yielded $NHNH_2$ intermediate, which requires 0.69 eV, and the subsequent release of the first NH_3 molecule resulted in a significant drop in energy by 1.59 eV, suggesting the formation of = NH on the surface as reported in previous studies.[31] The final hydrogenation steps leading to the release of the second NH_3 molecules occur with the release of energy, as revealed by the free energy profile presented in Figure 4b. Albeit the $CuBi_2O_4(211)$ surface appears to catalyze the formation of NH_3 molecules, the energetics of the first hydrogenation step (N_2 to N_2H), which is the rate-limiting step, limits the production of NH_3 owing to the $E_{barrier}$ of 0.26 eV, in contrast to the C−N coupling reaction. Thus, the catalyst effectively promotes the facile production of urea from CO_2 and N_2 molecules while small amounts of NH_3 are formed, in agreement with the experimental results.

CONCLUSIONS

This work presents the formation of urea starting from N_2 and CO_2 under the aid of water microdroplets and a $CuBi_2O_4$ catalyst. We believe this is an essential advance in demonstrating the power of water microdroplet chemistry. Multiple urea formation steps, including N_2 absorption, N≡N bond cleavage, nitrogen hydrogenation, and C−N bond formation, were processed in the liquid/gas, gas/solid, and liquid/solid interfaces at the submillisecond time scale without harsh conditions in temperature and high pressure and with no external applied voltage. The catalytic system has been operated for roughly 1 h with no apparent change in urea production rate. Water microdroplets are essential to causing this process occur. It is believed that the water microdroplet interface donates protons and electrons to cause the synthesis of urea in contact with the $CuBi_2O_4$ catalyst. It remains to be investigated whether this catalyst is an optimum choice and how long it can be operated without any degradation. How promising this synthesis might be for urea production on an industrial scale is presently unestablished. We believe that this requires further work on scaling water microdroplet chemistry.

ASSOCIATED CONTENT

Supporting Information

The Supporting Information is available free of charge at https://pubs.acs.org/doi/10.1021/jacs.3c10784.

Method and more detailed results, including a photo of the ultrasonic spray coupling with the mass spectrometer, mass spectra of negative control experiments for the urea formation test, contact angle of a drop of water (2 μL) on the $CuBi_2O_4$-coated mesh, ^{13}C NMR spectra of collected urea sample solution and the urea standard, optimization of the spray system to achieve the highest urea production, charging process of the $CuBi_2O_4$ catalyst mesh when it is sprayed with $N_2(g)-CO_2(g)-H_2O(l)$ at a flow rate of 10 μL/min and a nebulizing pressure of 120 psi, and optimized structural pathway of the concerted mechanism (PDF)

AUTHOR INFORMATION

Corresponding Authors

Chanbasha Basheer − *Chemistry Department, King Fahd University of Petroleum and Minerals, Dhahran 31261, Saudi Arabia*; orcid.org/0000-0001-6105-2822; Email: cbasheer@kfupm.edu.sa

Richard N. Zare − *Department of Chemistry, Stanford University, Stanford, California 94305, United States*; orcid.org/0000-0001-5266-4253; Email: rnz@stanford.edu

Authors

Xiaowei Song − *Department of Chemistry, Stanford University, Stanford, California 94305, United States*; orcid.org/0000-0003-3611-2816

Yu Xia − *Department of Chemistry, Stanford University, Stanford, California 94305, United States*; orcid.org/0000-0001-7647-4921

Juan Li − *School of Physics and Technology, Wuhan University, Wuhan 430072, China*

Ismail Abdulazeez − *Chemistry Department, King Fahd University of Petroleum and Minerals, Dhahran 31261, Saudi Arabia;* orcid.org/0000-0001-8098-5433
Abdulaziz A. Al-Saadi − *Chemistry Department, King Fahd University of Petroleum and Minerals, Dhahran 31261, Saudi Arabia;* orcid.org/0000-0001-7007-357X
Mohammad Mofidfar − *Department of Chemistry, Stanford University, Stanford, California 94305, United States*
Mohammed Altahir Suliman − *Chemistry Department, King Fahd University of Petroleum and Minerals, Dhahran 31261, Saudi Arabia*

Complete contact information is available at: https://pubs.acs.org/10.1021/jacs.3c10784

Author Contributions

[‖]X.S. and C.B. contributed equally.

Notes

The authors declare no competing financial interest.

■ ACKNOWLEDGMENTS

C.B. would like to acknowledge the Deanship of Research Oversight and Coordination at KFUPM for the sustainable Future Consortium grant SUFC2303. This work was supported by the Air Force Office of Scientific Research through the Multidisciplinary University Research Initiative (MURI) program (AFOSR FA9550-21-1-0170).

■ REFERENCES

(1) Antonetti, E.; Iaquaniello, G.; Salladini, A.; Spadaccini, L.; Perathoner, S.; Centi, G. Waste-to-chemicals for a circular economy: the case of urea production (waste-to-urea). *ChemSusChem* **2017**, *10*, 912−920.
(2) Barzagli, F.; Mani, F.; Peruzzini, M. From greenhouse gas to feedstock: formation of ammonium carbamate from CO_2 and NH_3 in organic solvents and its catalytic conversion into urea under mild conditions. *Green Chem.* **2011**, *13*, 1267−1274.
(3) Bernhard, A. M.; Peitz, D.; Elsener, M.; Wokaun, A.; Kröcher, O. Hydrolysis and thermolysis of urea and its decomposition byproducts biuret, cyanuric acid and melamine over anatase TiO_2. *Appl. Catal., B* **2012**, *115*−*116*, 129−137.
(4) Service, R. F. New recipe produces ammonia from air, water, and sunlight. *Science* **2014**, *345*, 610.
(5) Yan, X.; Liu, D.; Cao, H.; Hou, F.; Liang, J.; Dou, S. X. Nitrogen reduction to ammonia on atomic-scale active sites under mild conditions. *Small Methods* **2019**, *3*, 1800501.
(6) Lv, C.; Zhong, L.; Liu, H.; Fang, Z.; Yan, C.; Chen, M.; Kong, Y.; Lee, C.; Liu, D.; Li, S.; Liu, J.; et al. Selective electrocatalytic synthesis of urea with nitrate and carbon dioxide. *Nat. Sustain.* **2021**, *4*, 868−876.
(7) Srinivas, B.; Kumari, V. D.; Sadanandam, G.; Hymavathi, C.; Subrahmanyam, M.; De, B. R. Photocatalytic synthesis of urea from in situ generated ammonia and carbon dioxide. *Photochem. Photobiol.* **2012**, *88*, 233−241.
(8) Chen, S.; Perathoner, S.; Ampelli, C.; Mebrahtu, C.; Su, D.; Centi, G. Room-temperature electrocatalytic synthesis of NH_3 from H_2O and N_2 in a gas-liquid-solid three-phase reactor. *ACS Sustain. Chem. Eng.* **2017**, *5*, 7393−7400.
(9) Chen, L.; Wang, J.; Li, X.; Zhao, C.; Hu, X.; Wu, Y.; He, Y. A novel Z-scheme Bi-Bi_2O_3/$KTa_{0.5}$ $Nb_{0.5}O_3$ heterojunction for efficient photocatalytic conversion of N_2 to NH_3. *Inorg. Chem. Front.* **2022**, *9*, 2714−2724.
(10) Zhu, X.; Zhou, X.; Jing, Y.; Li, Y. Electrochemical synthesis of urea on MBenes. *Nat. Commun.* **2021**, *12*, 4080.
(11) Bao, D.; Zhang, Q.; Meng, F. L.; Zhong, H. X.; Shi, M. M.; Zhang, Y.; Yan, J. M.; Jiang, Q.; Zhang, X. B. Electrochemical reduction of N_2 under ambient conditions for artificial N_2 fixation and renewable energy storage using N_2/NH_3 cycle. *Adv. Mater.* **2017**, *29*, 1604799.
(12) Xu, S.; Ding, Y.; Du, J.; Zhu, Y.; Liu, G.; Wen, Z.; Liu, X.; Shi, Y.; Gao, H.; Sun, L.; Li, F. Immobilization of Iron Phthalocyanine on Pyridine-Functionalized Carbon Nanotubes for Efficient Nitrogen Reduction Reaction. *ACS Catal.* **2022**, *12*, 5502−5509.
(13) Liu, Y.; Tu, X.; Wei, X.; Wang, D.; Zhang, X.; Chen, W.; Chen, C.; Wang, S. C-Bound or O-Bound Surface: Which One Boosts Electrocatalytic Urea Synthesis? *Angew. Chem., Int. Ed.* **2023**, *62*, No. e202300387.
(14) Liu, B.; Xie, Y.; Wang, X.; Gao, C.; Chen, Z.; Wu, J.; Meng, H.; Song, Z.; Du, S.; Ren, Z. Copper-triggered delocalization of bismuth p-orbital favours high-throughput CO2 electroreduction. *Appl. Catal., B* **2022**, *301*, 120781.
(15) Chen, C.; Zhu, X.; Wen, X.; Zhou, Y.; Zhou, L.; Li, H.; Tao, L.; Li, Q.; Du, S.; Liu, T.; Yan, D.; et al. Coupling N_2 and CO_2 in H_2O to synthesize urea under ambient conditions. *Nat. Chem.* **2020**, *12*, 717−724.
(16) Song, X.; Basheer, C.; Zare, R. N. Making ammonia from nitrogen and water microdroplets. *Proc. Natl. Acad. Sci. U.S.A.* **2023**, *120*, No. e2301206120.
(17) Liu, B.; Xie, Y.; Wang, X.; Gao, C.; Chen, Z.; Wu, J.; Meng, H.; Song, Z.; Du, S.; Ren, Z. Copper-triggered delocalization of bismuth p-orbital favours high-throughput CO2 electroreduction. *Appl. Catal., B* **2022**, *301*, 120781.
(18) Hao, Q.; Liu, C.; Jia, G.; Wang, Y.; Arandiyan, H.; Wei, W.; Ni, B. J. Catalytic reduction of nitrogen to produce ammonia by bismuth-based catalysts: state of the art and future prospects. *Mater. Horiz.* **2020**, *7*, 1014−1029.
(19) Chen, X.; Xia, Y.; Zhang, Z.; Hua, L.; Jia, X.; Wang, F.; Zare, R. N. Hydrocarbon Degradation by Contact with Anoxic Water Microdroplets. *J. Am. Chem. Soc.* **2023**, *145*, 21538−21545.
(20) Colussi, A. J. Mechanism of hydrogen peroxide formation onsprayed water microdroplets. *J. Am. Chem. Soc.* **2023**, *145*, 16315−16317.
(21) Xing, D.; Meng, Y.; Yuan, X.; Jin, S.; Song, X.; Zare, R. N.; Zhang, X. Capture of Hydroxyl Radicals by Hydronium Cations in Water Microdroplets. *Angew. Chem., Int. Ed.* **2022**, *61*, No. e202207587.
(22) Hao, H.; Leven, I.; Head-Gordon, T. Can electric fields drive chemistry for an aqueous microdroplet? *Nat. Commun.* **2022**, *13*, 280.
(23) Xiong, H.; Lee, J. K.; Zare, R. N.; Min, W. Strong electric field observed at the interface of aqueous microdroplets. *J. Phys. Chem. Lett.* **2020**, *11*, 7423−7428.
(24) Chen, B.; Xia, Y.; He, R.; Sang, H.; Zhang, W.; Li, J.; Chen, L.; Wang, P.; Guo, S.; Yin, Y.; Hu, L.; Song, M.; Liang, Y.; Wang, Y.; Jiang, G.; Zare, R. N. Water-solid contact electrification causes hydrogen peroxide production from hydroxyl radical recombination in sprayed microdroplets. *Proc. Natl. Acad. Sci. U.S.A.* **2022**, *119*, 2209056119.
(25) Xue, G.; Xu, Y.; Ding, T.; Li, J.; Yin, J.; Fei, W.; Cao, Y.; Yu, J.; Yuan, L.; Gong, L.; Chen, J.; Deng, S.; Zhou, J.; Guo, W. Water-evaporation-induced electricity with nanostructured carbon materials. *Nat. Nanotechnol.* **2017**, *12*, 317−321.
(26) Lin, S.; Chen, X.; Wang, Z. L. Contact electrification at the liquid-solid interface. *Chem. Rev.* **2022**, *122*, 5209−5232.
(27) Zhou, Z.; Yan, X.; Lai, Y. H.; Zare, R. N. Fluorescence polarization anisotropy in microdroplets. *J. Phys. Chem. Lett.* **2018**, *9*, 2928−2932.
(28) Song, X.; Meng, Y.; Zare, R. N. Spraying water microdroplets containing 1, 2, 3-triazole converts carbon dioxide into formic acid. *J. Am. Chem. Soc.* **2022**, *144*, 16744−16748.
(29) Qiu, L.; Cooks, R. G. Simultaneous and Spontaneous Oxidation and Reduction in Microdroplets by the Water Radical Cation/Anion Pair. *Angew. Chem., Int. Ed.* **2022**, *61*, No. e202210765.
(30) Lee, J. K.; Samanta, D.; Nam, H. G.; Zare, R. N. Micrometer-sized water droplets induce spontaneous reduction. *J. Am. Chem. Soc.* **2019**, *141*, 10585−10589.

(31) Gong, C.; Li, D.; Li, X.; Zhang, D.; Xing, D.; Zhao, L.; Yuan, X.; Zhang, X. Spontaneous reduction-induced degradation of viologen compounds in water microdroplets and its inhibition by host-guest complexation. *J. Am. Chem. Soc.* **2022**, *144*, 3510−3516.
(32) Chen, H.; Wang, R.; Xu, J.; Yuan, X.; Zhang, D.; Zhu, Z.; Marshall, M.; Bowen, K.; Zhang, X. Spontaneous reduction by one electron on water microdroplets facilitates direct carboxylation with CO_2. *J. Am. Chem. Soc.* **2023**, *145*, 2647−2652.
(33) Jin, S.; Chen, H.; Yuan, X.; Xing, D.; Wang, R.; Zhao, L.; Zhang, D.; Gong, C.; Zhu, C.; Gao, X.; Chen, Y.; Zhang, X. The spontaneous electron-mediated redox processes on sprayed water microdroplets. *JACS Au* **2023**, *3*, 1563−1571.
(34) Yuan, X.; Zhang, D.; Liang, C.; Zhang, X. Spontaneous reduction of transition metal ions by one electron in water microdroplets and the atmospheric implications. *J. Am. Chem. Soc.* **2023**, *145*, 2800−2805.
(35) Ruiz-Lopez, M. F.; Francisco, J. S.; Martins-Costa, M. T.; Anglada, J. M. Molecular reactions at aqueous interfaces. *Nat. Rev. Chem* **2020**, *4*, 459−475.
(36) Yuan, M.; Chen, J.; Bai, Y.; Liu, Z.; Zhang, J.; Zhao, T.; Shi, Q.; Li, S.; Wang, X.; Zhang, G. Electrochemical C-N coupling with perovskite hybrids toward efficient urea synthesis. *Chem. Sci.* **2021**, *12*, 6048−6058.

https://doi.org/10.1021/jacs.3c10784
J. Am. Chem. Soc. 2023, 145, 25910−25916